Primary cilia and the exocyst are linked to urinary extracellular vesicle production and content

Received for publication, May 9, 2019, and in revised form, October 29, 2019 Published, Papers in Press, November 6, 2019, DOI 10.1074/jbc.RA119.009297

Xiaofeng Zuo[‡], Sang-Ho Kwon[§], Michael G. Janech[¶], Yujing Dang[‡], Steven D. Lauzon[‖], Ben Fogelgren[**], Noemi Polgar[**], and Joshua H. Lipschutz[‡ ‡‡1]

From the [‡]Department of Medicine, Medical University of South Carolina, Charleston, South Carolina 29425, the [§]Department of Cellular Biology and Anatomy, Augusta University, Augusta, Georgia 30912, the [¶]Department of Biology, College of Charleston, Charleston, South Carolina 29424, the [‖]Department of Public Health Sciences, Medical University of South Carolina, Charleston, South Carolina 29425, the [**]Department of Anatomy, Biochemistry, and Physiology, University of Hawaii at Manoa, Honolulu, Hawaii 96813, and the [‡‡]Department of Medicine, Ralph H. Johnson Veterans Affairs Medical Center, Charleston, South Carolina 29425

Edited by Phyllis I. Hanson

The recently proposed idea of "urocrine signaling" hypothesizes that small secreted extracellular vesicles (EVs) contain proteins that transmit signals to distant cells. However, the role of renal primary cilia in EV production and content is unclear. We previously showed that the exocyst, a highly conserved trafficking complex, is necessary for ciliogenesis; that it is present in human urinary EVs; that knockdown (KD) of exocyst complex component 5 (EXOC5), a central exocyst component, results in very short or absent cilia; and that human EXOC5 overexpression results in longer cilia. Here, we show that compared with control Madin-Darby canine kidney (MDCK) cells, EXOC5 overexpression increases and KD decreases EV numbers. Proteomic analyses of isolated EVs from EXOC5 control, KD, and EXOC5-overexpressing MDCK cells revealed significant alterations in protein composition. Using immunoblotting to specifically examine the expression levels of ADP-ribosylation factor 6 (ARF6) and EPS8-like 2 (EPS8L2) in EVs, we found that EXOC5 KD increases ARF6 levels and decreases EPS8L2 levels, and that EXOC5 overexpression increases EPS8L2. Knockout of intraflagellar transport 88 (IFT88) confirmed that the changes in EV number/content were due to cilia loss: similar to EXOC5, the IFT88 loss resulted in very short or absent cilia, decreased EV numbers, increased EV ARF6 levels, and decreased Eps8L2 levels compared with IFT88-rescued EVs. Compared with control animals, urine from proximal tubule-specific EXOC5-KO mice contained fewer EVs and had increased ARF6 levels. These results indicate that perturbations in exocyst and primary cilia affect EV number and protein content.

Primary cilia, found at the surface of many cell types, are sensory organelles known to perceive chemical (*e.g.* Hedgehog) and mechanical (*e.g.* fluid flow) signals. Defects in primary cilia lead to a number of human diseases termed ciliopathies. Ciliopathies can affect the kidney, where mutations that lead to disruption of ciliary structure and/or function result in autosomal dominant polycystic kidney disease (ADPKD), autosomal recessive PKD (ARPKD), and nephronophthisis, which are caused by mutations in the ciliary proteins polycystin-1 (1–3), polycystin-2 (3, 4), fibrocystin (5–7), and nephrocystins (8), respectively. Cystic overgrowth in PKD leads to destruction of the kidney architecture and renal failure (9). Although PKD is the fourth leading cause of end-stage kidney disease, accounting for ~5% of all end-stage kidney disease cases in the United States (10), the molecular mechanisms linking ciliary mutations to the cystic phenotype remain unclear.

Small membrane-bound extracellular vesicles (EV)[2] released via multivesicular bodies into the extracellular environment (called exosomes) (11) mediate cell-cell communication and affect signal transduction in recipient cells in both normal and pathological conditions. For example, platelet-derived exosomes regulate coating events (12), exosomes from intestinal epithelia activate the mucosal system (13), whereas tumor-derived exosomes transfer oncogenic receptors to receiving cells (14). In the kidney, and other organs, exosomes have also been suggested to carry disease-specific biomarkers (*e.g.* for acute kidney injury, chronic kidney disease, podocyte injury, cancers, and PKD (15–18)).

This work was supported in part by Veterans Affairs Merit Award I01 BX000820 (to J. H. L), National Institutes of Health Grant P30DK074038 (to J. H. L.), the Dialysis Clinic, Inc grant (to M. G. J. and J. H. L.), American Heart Association AWRP Winter 2017 Collaborative Sciences Award (to J. H. L.), and National Institutes of Health Grant 3UL1 TR001450 (to S. D. L.) to the South Carolina Clinical and Translational Research Institute. The authors declare that they have no conflicts of interest with the contents of this article. The content is solely the responsibility of the authors and does not necessarily represent the official views of the National Institutes of Health.

The proteomic data were deposited in the ProteomeXchange Database under accession number PXD013549.

This article contains Figs. S1–S4.

[1] To whom correspondence should be addressed: Medical University of South Carolina, 96 Jonathan Lucas St., CSB 829, Charleston, SC 29425. Tel.: 843-792-7659; Fax: 843-792-8399; E-mail: Lipschut@musc.edu.

[2] The abbreviations used are: EV, extracellular vesicle; PKD, polycystic kidney disease; MAPK, mitogen-activated protein kinase; MDCK, Madin-Darby canine kidney; EGFR, epidermal growth factor receptor; Eps8L2, epidermal growth factor receptor kinase substrate 8-like protein 2; MDCK, Madin-Darby canine kidney cells; EM, electron microscopy; BisTris, 2-[bis(2-hydroxyethyl)amino]-2-(hydroxymethyl)propane-1,3-diol; DAPI, 4′,6-diamidino-2-phenylindole; ERK, extracellular signal-regulated kinase; Ift88, intraflagellar transport 88; KO, knock-out; KD, knockdown; OE, overexpressing.

Over the past several years, EVs have been shown to be released from flagella and cilia (termed ectosomes). The unicellular alga *Chlamydomonas* achieves timely degradation of its mother cell wall, a type of extracellular matrix, through the budding of EVs containing a proteolytic enzyme directly from the membranes of its flagella (19). Another study showed that *Caenorhabditis elegans*-ciliated sensory neurons shed and release EVs containing polycystins LOV-1, the PKD-1 *C. elegans* ortholog (20), and PKD-2, and that these EVs were abundant in the lumen surrounding the cilium (21). Furthermore, electron microscopy (EM) and genetic analysis indicated that EV biogenesis occurred via budding from the plasma membrane at the ciliary base, and not via fusion of multivesicular bodies, and that intraflagellar transport and the ciliary protein KLP-6 were required for release of PKD-2–containing EVs. The EVs isolated from WT animals induced male tail-chasing behavior, whereas EVs isolated from klp-6 mutant animals lacking PKD-2 did not, indicating that environmentally released EVs play a role in communication and mating-related behaviors (21). Finally, it was recently shown, in murine inner medullary collecting duct (IMCD3) kidney cells, that, when activated, G protein–coupled receptors fail to undergo retrieval from cilia back into the cell. These G protein–coupled receptors concentrate into membranous buds at the tips of cilia before release into ectosomes, and hedgehog-dependent ectocytosis regulates ciliary signaling (22). Given the growing evidence of the existence and biological importance of ectosomes, the question of how they are regulated within the cell arises. We hypothesize that the exocyst complex and primary cilia play a critical role in their regulation.

The exocyst is a ~750–kDa octameric protein complex initially identified in *Saccharomyces cerevisiae*, and is highly conserved from yeast to mammals (23, 24). The mammalian exocyst is comprised of Exoc1–8 (previously called as Sec3, Sec5, Sec6, Sec8, Sec10, Sec15, Exo70, and Exo84) (23) and is best known for its role in targeting and docking vesicles carrying membrane proteins from the trans-Golgi network (25). Importantly, we showed in renal tubule cells that exocyst components are localized to primary cilia (26), that the exocyst is required for ciliogenesis (27), that Exoc5-containing vesicles are seen by EM gold microscopy at the tip and sides of primary cilia (27) (Fig. S1), that the exocyst genetically interacts with polycystin-2 in zebrafish (28, 29), and that kidney-specific knockout of Exoc5 leads to renal cystogenesis (30, 31). We and others have shown that the exocyst regulates the MAPK pathway via EGFR (29, 32, 33). Most recently, by mutating the V*XP*X ciliary targeting sequence in Exoc5, we confirmed that the ciliary function of the exocyst is responsible for the phenotypic changes following Exoc5 KD/KO (34). Mutations in an exocyst protein were shown to cause Joubert syndrome, a nephronophthisis form of PKD, in a human family (35). EVs carry many *cilia-specific* membrane proteins, including the exocyst, regulators of the exocyst (*e.g.* CDC42), polycystin-2, the protein product of *PKD2*, as well as ciliary membrane proteins such as Smoothened (36). As noted, we have also shown, using EM (27, 36), that cilia interact with EVs. Thus, a link between the exocyst, primary cilia, and cystic kidney disease has been established.

Given that understanding the mechanisms that mediate cilia/EV interactions could be critical to elucidating the biology linking cilia to renal disease, especially PKD, we explored the link between renal primary cilia, urinary EVs, and the exocyst. Here, we show that inhibiting ciliogenesis by Exoc5 knockdown and intraflagellar transport protein 88 (Ift88) knockout leads to a significant decrease in EV number and a change in protein content. EXOC5 overexpression, on the other hand, leads to an increase in EV number, as well as a change in EV protein content. Rescue of the cilia phenotype in Ift88 KO cells with exogenous Ift88 reverses these changes.

Results

EV number is changed following Exoc5 perturbation

To determine how loss of cilia changes the number and/or composition of EVs, 1.0×10^5 cells of Exoc5 OE, Exoc5 KD, and control Madin-Darby canine kidney (MDCK) cells were seeded in 12-well Transwell dishes and grown for 10 days with exosome-free medium changed daily. The conditioned medium was collected after the final change. Following harvesting of the medium, purification of the EVs was achieved by a series of ultracentrifugation steps as described under "Materials and Methods." The nanoparticle tracking analysis was performed with the ZetaView Nanoparticle Tracking Analyzer using the settings described under "Materials and Methods." The ZetaView analysis showed that media from all the cellular conditions (EXOC5 OE, Exoc5 KD, and control MDCK cells) yielded 50–150 nm EVs (Fig. 1*A*). The number of EVs/ml produced by the Exoc5 KD cells was significantly less, whereas the number of EVs/ml was significantly greater for the EXOC5 OE cells, compared with control MDCK cells (Fig. 1*B*). Using EM, we confirmed the 50–150 nm size of the EVs (Fig. 1*C*).

Proteomic analysis of EV proteins following Exoc5 perturbation

To study how Exoc5 changes the composition of EVs, we grew large amounts (nine 15-cm plastic dishes for each replicate) of EXOC5 OE, Exoc5 KD, and control MDCK cells in minimal essential media supplemented with 5% exosome-free FBS, and collected the protein lysate for MS, which was performed as described under "Materials and Methods."

Determination of the protein composition of extracellular vesicles following Exoc5 perturbation

Mass spectrometry was performed as described under "Materials and Methods." We found that Exoc5 perturbation significantly affected the protein composition of EVs as can be seen by the complete segregation of samples in the dendrogram (Fig. 2*A*), principal components analysis (Fig. 2*B*), and heat map of differentially expressed proteins (Fig. 2*C*). The proteomic data were deposited in the ProteomeXchange Database under accession number PXD013549.

Confirmation of the proteomic results using Western blotting

To confirm the MS results, we performed Western blot analysis on two representative proteins that were interesting candi-

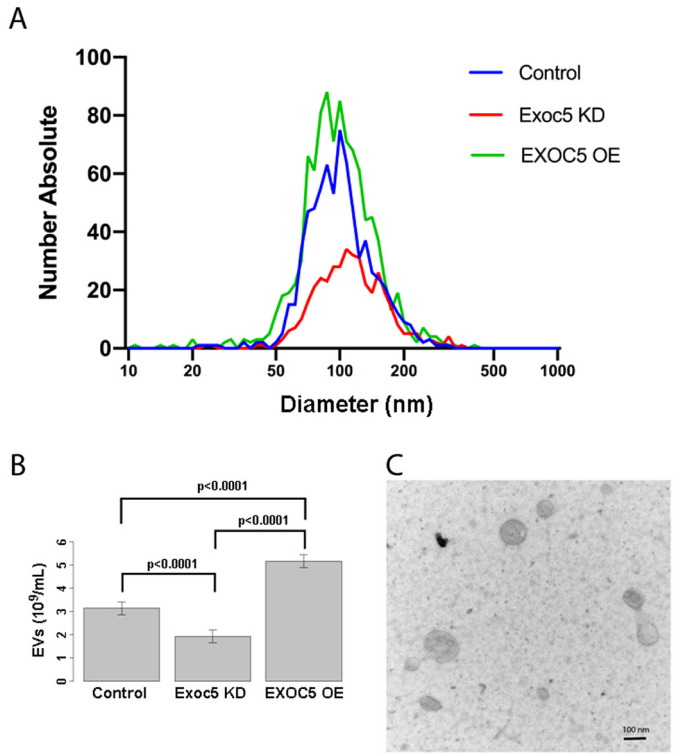

Figure 1. EV number is increased in EXOC5 OE, and decreased in Exoc5 KD, compared with control MDCK cells. *A,* the size and number of EVs isolated from stable EXOC5 overexpressing (*OE*), Exoc5 knockdown (*KD*), and control MDCK cells, using a standard ultracentrifugation procedure as described under "Materials and Methods," were measured with a ZetaView scanner. The uniform size of the EVs demonstrated the purity and consistency of the preparation, and the size (50–150 nm) suggested these were exosomes or ectosomes, which is the EV population we were targeting. *B,* quantification demonstrated that there were significantly more EVs from EXOC5 OE, and significantly less EVs from Exoc5 KD, compared with EVs from control MDCK cells. This experiment was repeated three times with similar results. *Error bars* represent 95% confidence intervals. *C,* EM confirmed the 50–150 nm size of the EVs.

dates based on the literature. We chose to investigate ADP-ribosylation factor 6 (Arf6), a small GTPase that has been shown to regulate Exoc5 (37). We also focused on the epidermal growth factor receptor kinase substrate 8-like protein 2 (Eps8L2), and Erk, as we, and others, have shown that the exocyst regulates the MAPK pathway via EGFR (29, 32, 33). Importantly, Arf6 and Eps8 (although not Eps8L2) have previously been found in human urinary EVs (38), and in primary cilia (39). We grew Exoc5 KD, EXOC5 OE, and control MDCK cells, and isolated EVs using ultracentrifugation as described under "Materials and Methods." Western blotting of lysate from the EVs showed that Exoc5 was virtually absent in Exoc5 KD cell EVs, and significantly increased in EXOC5 OE cell EVs, compared with EVs from control MDCK cells (Fig. 3, *A* and *B*). As would be expected from our previous results showing loss of Exoc4 with KD of Exoc5 (27), we found significantly less Exoc4 in EVs from Exoc5 KD cells (all Western blotting results were measured in normalized arbitrary units), compared with EVs from control MDCK cells. Similar to the MS results (Exoc5 KD, 8 ± 1; EXOC5 OE, 6 ± 0; MDCK WT, 4 ± 3.5) there was significantly more Arf6 in EVs from Exoc5 KD cells, compared with EVs from control MDCK and EXOC5 OE cells, and no significant difference in Arf6 between EVs from EXOC5 OE and MDCK WT cells. Also similar to the MS results (Exoc5 KD, 0 ± 0; EXOC5 OE, 33 ± 11.5; MDCK WT, 9.3 ± 3.5), there was significantly less Eps8L2 in EVs from Exoc5 KD cells, compared with EVs from control MDCK and EXOC5 OE cells, and more Eps8L2 in EVs from EXOC5 OE compared with MDCK WT cells (Fig. 3, *A* and *B*). Finally, similar to our previous results showing that Exoc5 inhibition increases phosphorylated (active) Erk (pErk) (29), we found that Exoc5 KD increased pErk, whereas EXOC5 OE decreased pErk, compared with MDCK control cell EVs (Fig. 3, *A* and *B*).

We also used a second EV isolation method, the Total Exosome Isolation Kit (Invitrogen), and found similar results. 1) significantly increased levels of Exoc5 in EVs from EXOC5 OE, and decreased levels of Exoc5 in EVs from Exoc5 KD, compared with EVs from control MDCK cells. 2) Significantly less Eps8L2 in EVs from Exoc5 KD cells, compared with EVs from control MDCK and EXOC5 OE cells, and more Eps8L2 in EVs from EXOC5 OE compared with MDCK WT cells. 3) Significantly more Arf6 in EVs from Exoc5 KD cells, compared with EVs from control MDCK and EXOC5 OE cells, and no significant difference in Arf6 between EVs from EXOC5 OE and MDCK WT cells (Fig. S2).

Importantly, there were no differences in Arf6 and Eps8L2 levels in whole cell lysate from Exoc5 OE, KD, and control MDCK cells (Fig. S3). The Arf6 and Eps8L2 levels in EVs seen by Western blotting using both isolation methods were similar to what we found using MS, thereby supporting the validity of the proteomics results.

Investigation of a second cell line lacking primary cilia

Given that the exocyst has been shown by us and others (40–43) to perform multiple cellular functions, to confirm that our EV results were a cilia-related effect, we grew stable Ift88 KO and rescue cells (44) as described under "Materials and Methods." We first confirmed that the Ift88 cells lacked cilia, whereas Ift88 rescue cells have primary cilia (Fig. 4*A*). We then confirmed by Western blotting that the Ift88 KO cells contained no IFT88 protein, and that the Ift88 rescue cells had IFT88 (Fig. 4*B*). The Ift88 KO and rescue cells were then grown to 100% confluence, and the media were collected 5 days later, with the media changed every 2 days. The conditioned media was collected 24 h after the final media change, and EVs were purified using ultracentrifugation as described under "Materials and Methods." Similar to Exoc5 KD MDCK cells, there was significantly less EVs per cell produced by the Ift88 KO cells, as compared with the Ift88 rescue cells (Fig. 4*C*). Analogous to what we found following perturbation of Exoc5, we found significantly more Arf6 in EVs from Ift88 KO cells, compared with EVs from Ift88 rescue cells, and less Eps8L2 in Ift88 KO cells, compared with Ift88 rescue cells. We also found increased pErk in EVs from Ift88 KO cells compared with EVs from Ift88 rescue cells (Fig. 4*D*). Overexpression of EXOC5 in the Ift88 KO cells did not change the number of EVs produced (Fig. S4), indicating that the decrease in EV production in Ift88 KO and Exoc5 KD cells was related to loss of primary cilia, and not parallel processes.

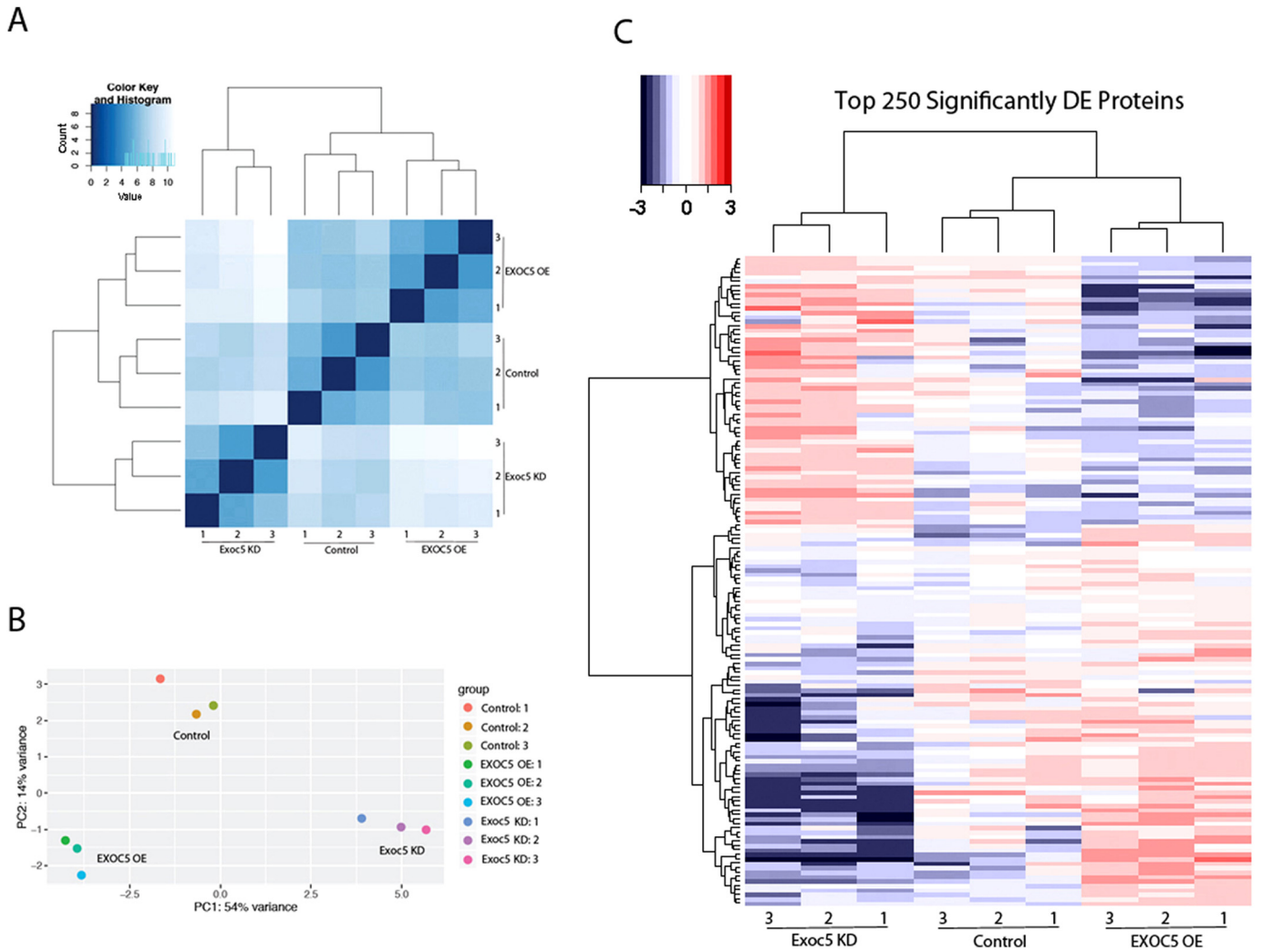

Figure 2. EVs from EXOC5 OE, Exoc5 KD, and control MDCK cells had significantly different protein content as determined by proteomic analysis. *A,* the dendrogram reveals that the experimental samples fall into three distinct groups: EXOC5-overexpressing (*OE*), Exoc5 knockdown (*KD*), and control MDCK cells. *B,* this panel shows a principal component analysis (PCA plot) of the same nine samples shown in the 2D plane spanned by their first two principal components. This plot allows visualization of the overall effect of experimental covariates and reveals the absence of batch effects. *C,* the top 250 differentially expressed (*DE*) proteins were plotted with the *blue* color denoting down-regulation, and the *red* color up-regulation. The heat map shows that all three samples in each condition are similar, and each of the three conditions are quite distinct.

Determination of Arf6 levels in EVs from the urine of proximal tubule-specific Exoc5 knockout mice

To determine whether similar events occurred *in vivo* following loss of Exoc5, we generated proximal tubule-specific knockout mice by crossing our tdTom-Exoc5fl/fl mice (30) with SLC34A-CreERT2 mice, which express Cre in the S1, S2, and part of the S3 segments of the proximal tubule when induced with tamoxifen (45). We first generated a male SLC34A-CreERT2;tdTom-Exoc5fl/+ mouse, and backcrossed this mouse against the tdTom-Exoc5fl/fl female mouse. In the first litter we obtained a target SLC34A-CreERT2;tdTom-Exoc5fl/fl mouse and a tdTom-Exoc5fl/fl control mouse, which was determined by genotyping at 21 days after birth using PCR. At age 7 weeks, we injected tamoxifen intraperitoneally for 3 days in a row into the Exoc5fl/fl control and SLC34A-CreERT2;tdTom-Exoc5fl/fl target mice, and collected urine using metabolic cages. Following urine collection, the mice were sacrificed. tdTomato has a lox-stop-lox cassette surrounding the Tomato reporter, allowing us to confirm Exoc5 knockout in the SLC34A-CreERT2; tdTom-Exoc5fl/fl mouse by tdTomato expression (*red color*, Fig. 5*A*) (46). Identical settings on the fluorescence microscope were used and no tdTomato expression was seen in the kidneys of the tdTom-Exoc5fl/fl mouse (Fig. 5*A*). Proximal tubule-specific KO was confirmed by coexpression of the tdTomato reporter and proximal tubule-specific *Lotus tetragonolobus* agglutinin marker (Fig. 5*B*). EVs were isolated from the urine by ultracentrifugation, and Western blotting was performed. Similar to the cell culture results, significantly more Arf6 was seen in EVs from the target SLC34A-CreERT2;tdTom-Exoc5fl/fl, compared with the control tdTom-Exoc5fl/fl mice (Fig. 5*C*). Also, similar to the cell culture results, pErk was significantly increased in EVs from the SLC34A-CreERT2;tdTom-Exoc5fl/fl target, compared with the control tdTom-Exoc5fl/fl mouse. Unlike the cell culture results, we did not see a difference in the level of Eps8L2 in EVs from the target SLC34ACreERT2; tdTom-Exoc5fl/fl compared with the control tdTom-Exoc5fl/fl

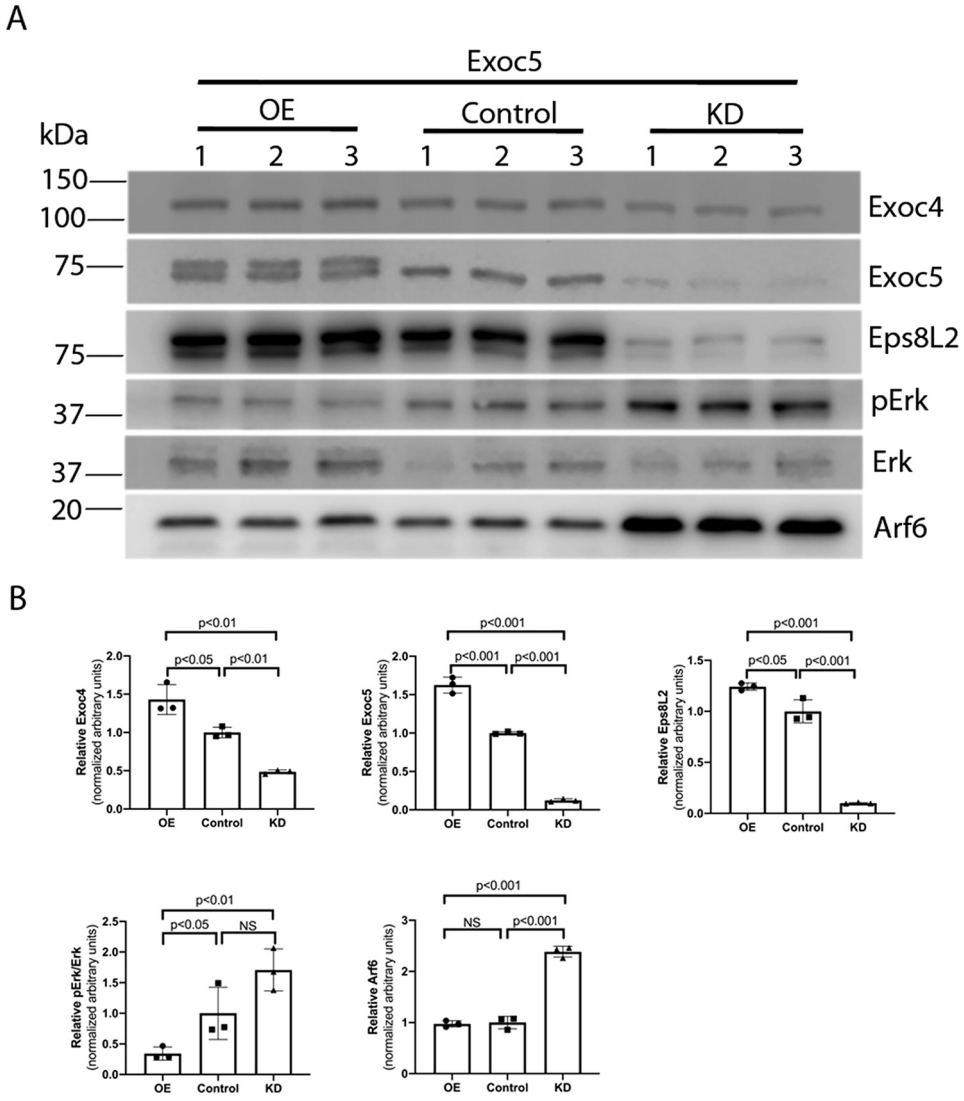

Figure 3. Confirmation of the proteomic results by Western blotting. *A,* equal amounts of EV proteins (2 μg per lane) from EXOC5 overexpressing (*OE*), Exoc5 knockdown (*KD*), and control MDCK cells were obtained using a series of ultracentrifugation steps as described under "Materials and Methods," and were run on a gel for Western blot analysis. *B,* quantification of the Western blotting data shows a significant decrease in Exoc5 protein in EVs from Exoc5 KD cells, and a significant increase in Exoc5 in EVs from EXOC5 OE cells, compared with EVs from control MDCK cells. There was also significantly less Exoc4 protein in EVs from Exoc5 KD, and increased Exoc4 in EVs from EXOC5 OE, compared with EVs from control cells. Importantly, there was a large increase in Arf6 in EVs from Exoc5 KD, compared with EVs from control and EXOC5 OE MDCK cells. There was also significantly less Eps8L2 in EVs from Exoc5 KD cells, compared with EVs from control MDCK cells, and more Eps8L2 in EVs from EXOC5 OE compared with control MDCK cells. Finally, there was significantly more phosphorylated (active) Erk (*pErk*) in EVs from Exoc5 KD cells, compared with EVs from control cells, and less pErk in EVs from EXOC5 OE compared with control MDCK cells. This experiment was repeated three times with similar results.

mouse. EVs in the urine likely come from all tubular segments, not just the proximal tubules where Exoc5 was deleted, which could explain the differences in the *in vivo* and *in vitro* results.

Discussion

We report here five principal findings, all of which are important for our understanding of urinary EV production. First, we show that primary cilia are necessary for the production/release of a significant subset of 50–150 nm EVs in renal tubular cells. Primary cilia are absent in Exoc5 KD cells, and longer cilia are found in EXOC5 OE cells (27). Primary cilia are also absent in Ift88 KO cells, and present in Ift88 rescue cells (44). In both Exoc5 KD and Ift88 KO cells, there were ~60% less EVs produced than in their respective controls. This is remarkable in that the primary ciliary membrane accounts for only ~0.2% of the total cell membrane (47). Furthermore, the number of EVs produced correlated with the length of the primary cilia with EXOC5 OE cells producing more EVs, and Exoc5 KD cells producing less EVs, compared with control MDCK cells.

Second, depending on the length of primary cilia, the content of the EVs was also different, as determined by MS and Western blotting analyses. This is seen on the dendrogram as complete segregation of protein content in EVs from EXOC5 OE (longer cilia), Exoc5 KD (short or absent cilia), and control MDCK cells. Western blotting confirmation of the MS results was performed for two proteins, Arf6 and Eps8L2. Similar to Exoc5 KD cells, there was more Arf6, and less Eps8L2, found in the EVs from Ift88 KO cells, compared with Ift88 rescue cells. Finally, there was more Arf6 in EVs from the urine of a homozygous proximal tubule-specific Exoc5 KO compared with a littermate

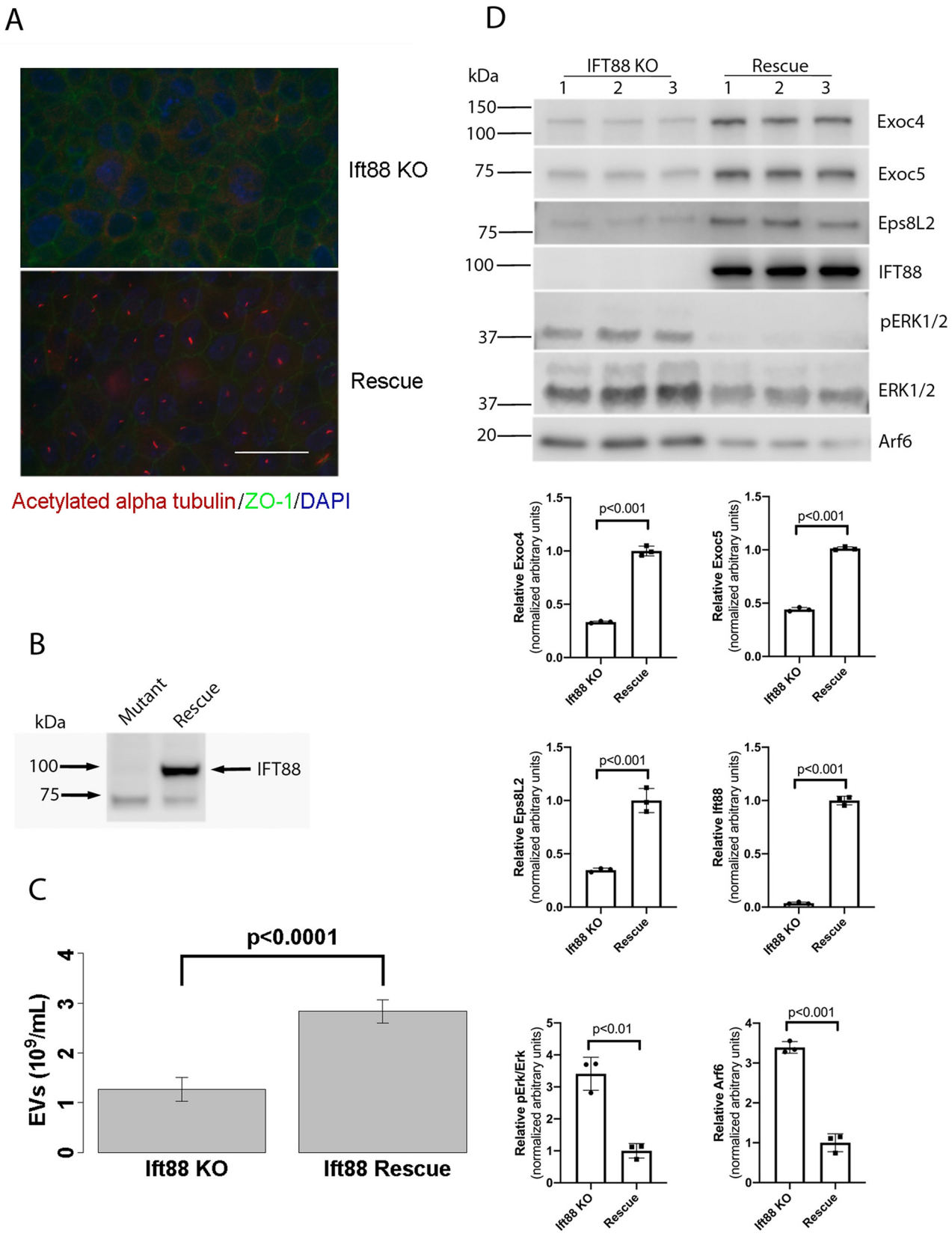

Figure 4. EV production is decreased in ciliary-deficient Ift88 KO cells and increased in the rescue cells. *A,* stable Ift88 knockout (*KO*) and Ift88 rescue mouse cells were grown on Transwell filters. As previously reported, Ift88 KO cells do not form cilia, whereas Ift88 rescue cells form cilia. *Bar* = 25 μm. *B,* Western blotting from the lysate of Ift88 KO and rescue cells, shows that Ift88 is absent in the KO cells, and present in the rescue cells. *C,* similar to what we found with the Exoc5-perturbed cells, the Ift88 KO cells produced significantly fewer EVs per cell than the Ift88 rescue cells. *Error bars* represent 95% confidence intervals. *D,* similar to the Exoc5 KD cells, there was significantly more Exoc4, Exoc5, Ift88, and Eps8L2 in EVs from Ift88 rescue compared with Ift88 KO cells. There was also significantly less Arf6 and phosphorylated (active) Erk (*pErk*) in EVs from Ift88 rescue compared with Ift88 KO cells.

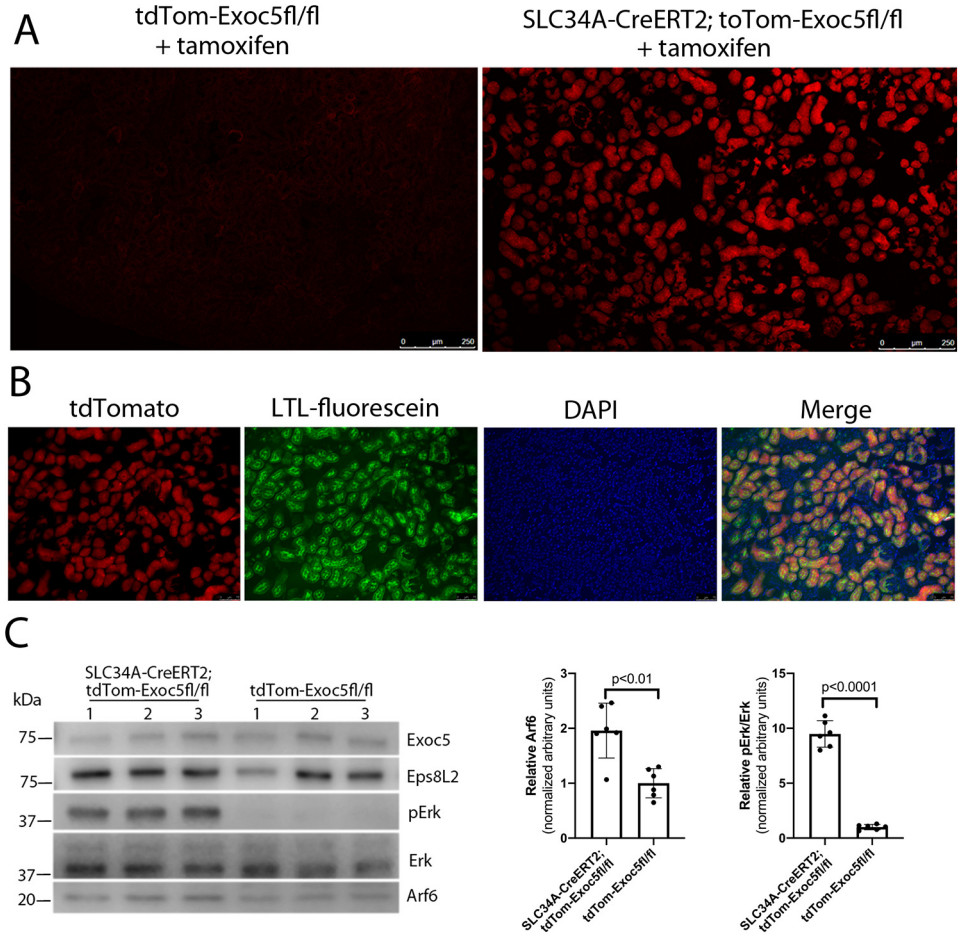

Figure 5. EVs from the urine of a homozygous proximal tubule-specific Exoc5 KO mouse contain more Arf6 and pErk, compared with urinary EVs from control mice. *A,* kidney sections from an SLC34A-CreERT2;tdTom-Exoc5fl/fl mouse exposed to tamoxifen show tdTomato expression (*red color*) in the tubules of SLC34A-CreERT2;tdTom-Exoc5fl/fl, but not in control, mice. This indicates activation of Cre and KO of Exoc5 in the SLC34A-CreERT2;tdTom-Exoc5fl/fl mice. *B,* co-staining with LTA-fluorescein demonstrates that the knockout of Exoc5 is occurring in the proximal tubules. *C* and *D,* quantification of the Western blotting data shows that there was significantly more Arf6 and phosphorylated (active) Erk (*pErk*) in EVs from SLC34A-CreERT2;tdTom-Exoc5fl/fl (homozygous proximal tubule-specific Exoc5 KO) compared with tdTom-Exoc5fl/fl (control) mice.

control mouse. A possible explanation is that Arf6 is packaged in exosomes that are secreted via multivesicular bodies, and this is independent of the ectosomes secreted from primary cilia. With loss of cilia, exosomes become a higher percentage of the EV population and, therefore, there are greater levels of Arf6 seen.

Third, we show that the exocyst is likely to be specifically involved in ciliary EV generation. There is a question of how the exocyst can be involved in so many different cellular processes. We, and others, have shown that the exocyst is found in most cell types and is involved in a wide variety of cellular processes, including: vesicular transport to the basolateral membrane (40, 41), primary ciliogenesis (27, 29, 46), protein synthesis in the endoplasmic reticulum (42, 43), and post-endocytic recycling (37). We and others have also shown that small GTPases from the Rab (48), Arf (37, 49), Rho (28, 50, 51), and Ral (52–55) families regulate the exocyst. We hypothesize that the many small GTPases, found at different locations in the cell, give the exocyst specificity of function. We have shown using cell culture, zebrafish, and kidney-specific knockout in mice that Cdc42 is found at the primary cilium and regulates the exocyst (28). Likewise, Tuba, a ciliary Cdc42 guanine nucleotide exchange factor, regulates the exocyst and is also necessary for ciliogenesis, cystogenesis, and tubulogenesis (56–58). We have similarly shown that Arl13b, a ciliary Arf family GTPase, regulates the exocyst (49). The fact that multiple small GTPases regulate the exocyst at the primary cilium, suggests that the exocyst, in addition to trafficking vesicles to the primary cilium, may have other function(s) in the primary cilium. One of these functions may be the secretion and/or retrieval of EVs. If the exocyst were only involved in trafficking vesicles carrying proteins necessary for ciliogenesis, one would expect to find it only at the base of the primary cilium; instead, we have shown that Exoc4 and -5 localize not only to the base of primary cilia, but all along the primary cilium and, indeed, in cilia-interacting EVs (27, 36). Additionally, we found that all eight members of the exocyst complex, as well as many regulatory GTPases, including Arf6, are present in human urinary EVs (36).

Fourth, we link the exocyst and EVs to Arf6, which has been shown to regulate the exocyst through Exoc5 to control post-endocytic recycling (37), a process that may also be involved in EV generation/retrieval. Arf6 and the exocyst have also been found in urinary EVs (38, 59). Indeed, we have previously shown that: 1) Arl13b, another Arf family member, in its GTP form,

regulates the exocyst; 2) arl13b and cdc42 genetically interact in zebrafish; and 3) knockout of Arl13b in mice leads to renal cystogenesis (49). Renal cystogenesis is also seen in kidney-specific Exoc5 knockout mice surviving for 30 days (30, 31).

Finally, we show that loss of Exoc5 results in phosphorylated (active) Erk being found in EVs. This is concordant with our previous studies in which we found that loss of exoc5 in zebrafish leads to increased pErk (29). We and others have also shown that the exocyst regulates the MAPK pathway via EGFR (29, 32, 33). Eps8L2 may be involved in this regulation, although it would likely be an inhibitor of the pathway, as Exoc5 KD and Ift88 KO lead to increased pERK and decreased Eps8L2.

In summary, we show here that the primary cilia and the exocyst are involved in EV generation in mammalian renal cells, that the exocyst, Arf6, and Eps8L2 may interact in EV generation (and possibly retrieval), and that the MAPK pathway is likely to be centrally involved in EV generation. These data, combined with the growing experimental evidence suggesting a biologically relevant role for cilia/EV interactions, supports a model whereby the exocyst is centrally involved in the regulation of cilia/EV interactions via Arf6 (Fig. 6). The fact that the exocyst complex is required for normal ciliogenesis (27), and that an exocyst mutation results in the Joubert nephronophthisis form of PKD in a human family (35), demonstrates the central role of the exocyst in regulating normal and pathogenic ciliogenesis, which now may also include cilia/EV interactions.

Materials and methods

Animal study approval

All animal studies were conducted per the protocols approved by the Medical University of South Carolina and/or Ralph H. Johnson VAMC Institutional Animal Care and Use Committee, and NIH guidelines for the Care and Use of Laboratory Animals. Treatment of mice, including housing, injections, and surgery was in accordance with the institutional guidelines.

Cell culture

Type II MDCK cells were used between passages 3 and 10. These cells were originally cloned by Dr. D. Louvard (European Molecular Biology Laboratory, Heidelberg, Germany) and came to us via Dr. K. Mostov, who obtained them from Dr. K. Matlin (University of Chicago, Chicago, IL). We previously generated myc-tagged human EXOC5 OE (41) and Exoc5 KD cells (27) from parent MDCK cells. All of these cell lines were cultured in modified Eagle's minimal essential medium containing Earl's balanced salt solution and glutamine supplemented with 5% exosome-free FBS, 100 units/ml of penicillin, and 100 μg/ml of streptomycin. Mouse Ift88 KO and rescue cells were obtained from the NIH P30 University of Alabama at Birmingham Hepatorenal Fibrocystic Diseases Core Center (HRFDCC). These cells were cultured in CD media (Dulbecco's modified Eagle's medium/F12, 10% exosome-free FBS, 1.3 μg/liter of sodium selenite, 1.3 μg/liter of 3,3′,5-triiodothyronine, 5 mg/liter of insulin, 5 mg/liter of transferrin, 2.5 mM glutamine, 5 μM dexamethasone, 100 units/ml of penicillin, 100 mg/ml of streptomycin, 10 units/ml of interferon-γ) at 33 °C and 5% CO_2.

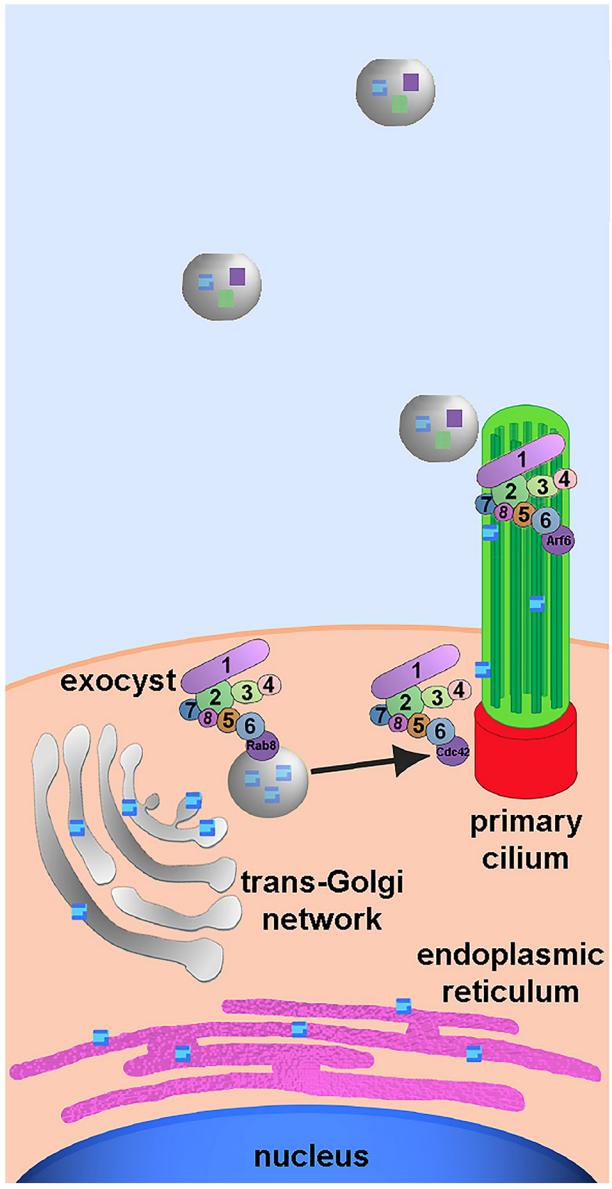

Figure 6. Model for how the exocyst is involved in EV secretion and/or retrieval via the primary cilium. Genes are transcribed into mRNA in the nucleus, and mRNA is translated into proteins in the endoplasmic reticulum. Proteins destined for the primary cilium are packaged in vesicles in the trans-Golgi network, and trafficked to the primary cilium by the exocyst complex. Exoc5 is a central exocyst member as it links Exoc6 (bound to the vesicle via the small GTPase Rab8) and the rest of the exocyst complex. The exocyst itself is targeted to the primary cilium by another small GTPase, Cdc42. Finally, the exocyst is involved in EV secretion and/or retrieval under the control of the ciliary and EV small GTPase Arf6.

EV isolation

For nanoparticle tracking analysis, 1.0×10^5 cells of Exoc5 OE, Exoc5 KD, and control MDCK cells were seeded in 12-well Transwell dishes and grown for 10 days with the medium changed daily. For proteomic analysis, we grew large amounts (nine 15-cm plastic dishes for each replicate) of EXOC5 OE, Exoc5 KD, and control MDCK cells. Cells were grown to 100% confluence, and conditioned media was harvested 5 days later, with the media changed every 2 days.

The conditioned media was collected 24 h after the final media change. Purification of the EVs was achieved by first

centrifuging the conditioned media at 3,000 × *g* for 15 min at 4 °C to remove large debris, and then collecting the supernatant. The supernatant was centrifuged at 12,000 × *g* for 40 min at 4 °C, and the remaining supernatant was again collected. The final supernatant was centrifuged at 143,000 × *g* for 70 min at 4 °C to obtain the EV pellet, which was washed with PBS to eliminate contaminating proteins, and centrifuged one last time at 143,000 × *g* for 70 min at 4 °C. The resulting pellet was resuspended in 150 μl of PBS.

For the second EV isolation method, EXOC5 OE, Exoc5 KD, and control MDCK cells were grown to confluence on plastic culture dishes in exosome-free medium, which was changed daily, for 5 days. The conditioned medium was collected and used to isolate EVs with the Total Exosome Isolation Kit (Invitrogen, catalog number 4478359) per the manufacturer's instructions.

Proteomic analysis of EV proteins by MS

To determine how Exoc5 changes the composition of EVs, samples (20 μg protein) for each condition (EXOC5 OE, Exoc5 KD, and control MDCK cells-all in triplicate) were sequentially digested with LysC (1:100) and trypsin (1:20) in sodium deoxycholate (60). Peptides were desalted with solid phase chromatography cartridges (Strata-x, Phenomenex). Peptides were resuspended in 0.1% formic acid and equal amounts (2 μg) were separated with a linear gradient of 5–50% buffer B (95% acetonitrile and 0.1% formic acid) at a flow rate of 200 nl/min on a C18-reversed phase column packed in-house with ReproSil-Pur, 120 C18-AQ, 1.9 μm of resin. A Dionex U3000 nano-LC chromatography system (Thermo Scientific) was on-line coupled to the Orbitrap Elite instrument (Thermo Scientific). Mass spectrometry data were acquired using a data-dependent strategy in the survey scan (400–1700 m/z). The resolution of the survey scan was ~60,000 at 400 m/z with a target value of 1e6 ions. Low resolution CID MS/MS spectra were acquired in the linear ion trap in normal CID scan mode. The maximum injection time for MS/MS was 100 ms. Dynamic exclusion was 120 s and early expiration was enabled. The isolation window for MS/MS fragmentation was set to 2 m/z.

Determination of the protein composition of extracellular vesicles following Exoc5 perturbation

The raw MS data were converted to .mgf files within Proteome Discoverer 1.4. Peptide data were searched using MASCOT (version 2.4) against the NCBI Canine proteome (NCBI annotation release 104), and a common repository of adventitious proteins, which also included green fluorescent protein (GFP). Carbamidomethyl modification was fixed for cysteine. Oxidation of methionine and peptide N-terminal pyroglutamate were selected as variable modifications. Parent ion mass tolerance was set to 30 ppm and fragment ion mass tolerance was set to 0.25 Da. Search data were imported to Scaffold Q+S and false discovery rate criteria (61) were applied at a level of 1% for both peptide and protein level assignments. Count data were analyzed using DEseq2 (62, 63). Fold-change estimation and hypothesis testing for differential expression of proteins/peptides was performed using the DESeq2 Bioconductor library (62–64). The false discovery rate was controlled at 10%.

Immunofluorescence staining

For immunofluorescence staining of MDCK cells grown on Transwell filters, the cells were directly fixed in 4% paraformaldehyde for 20 min at room temperature. The fixed cells were permeabilized for 15 min at 37 °C with 0.025% saponin in 1× PBS. After blocking with PFS buffer (0.025% saponin and 0.7% fish skin gelatin in 1× PBS), the cells were incubated with primary antibodies in the PFS buffer overnight at 4 °C, and secondary antibodies for 1 h at room temperature. After nuclear staining with DAPI, the cells were post-fixed in 4% paraformaldehyde, and mounted with a mounting medium (71-00-16, KPL).

Cell lysate

EXOC5 OE, Exoc5 KD, and control MDCK cells were grown to confluence on plastic culture dishes for 5 days. Cells were washed twice with cold PBS, lysed with RIPA buffer for 30 min on ice, then centrifuged for 15 min at 13,500 rpm at 4 °C, to obtain cell lysate for Western blot analysis.

Transfection

Ift88 KO cells were plated in 6-well dishes, 3×10^5 cells per well. The following day, when cell confluence reached 70–90%, 5 μg of DNA of pcDNA3 containing human EXOC5, or empty pcDNA3, plasmid was used with Lipofectamine LTX (Invitrogen, catalog number 15338030) to transfect the Ift88 KO cells. Transfected cells were washed twice and fed with 1.5 ml of fresh medium 24 h following the transfection. The conditioned media was collected 24 h after the media change and EVs were isolated by ultracentrifugation as described above. The cells in the 6-well dishes were then trypsinized, collected, and counted, and the cell number was used to normalize the EV concentration. Finally, the cells were lysed with RIPA buffer for Western blotting as described below.

Western blot analysis

The protein samples were separated on Bolt 4–12% BisTris gels (NW04125, Novex) and then transferred to a nitrocellulose membrane (LC2000, Novex). The membranes were blocked with 5% nonfat dry milk in 1× PBS containing 0.1% Tween 20 and incubated with primary antibodies overnight at 4 °C. After washing with 1× PBS containing Tween 20, the membranes were incubated with horseradish peroxidase-conjugated secondary antibodies for 1 h at room temperature. Finally, the membranes were exposed to a Western blotting chemiluminescence reagent (34095, Thermo), and imaged in Odyssey Fc Imaging System (LI-COR).

Antibodies

The primary antibodies used in this study were mouse monoclonal anti-acetylated α-tubulin (T6793, Sigma-Aldrich), anti-EXOC5, which we previously generated (27), anti-Arf6 (sc-7971, Santa Cruz), anti-Eps8L2 (GTX112158, GeneTex), anti-Erk (4696, Cell Signaling) anti-pErk (9101, Cell Signaling), anti-ZO1 (a gift from Dr. Keith Mostov), anti-glyceraldehyde-3-phosphate dehydrogenase (G8795, Sigma), anti-β-actin (GTX629630, GeneTex), and anti-Exoc4 (ADI-VAM-SV016, Enzo). The secondary anti-

bodies and stains we used were: Alexa Fluor 555, phalloidin (A34055, Invitrogen), goat anti-mouse/anti-rabbit horseradish peroxidase-conjugated secondary antibodies (115-035-003 for mouse and 111-035-003 for rabbit, Jackson ImmunoResearch Laboratories), fluorescein-labeled *L. tetragonolobus* lectin (LTL) (FL-1321, Vector) and DAPI.

Histological analysis

Frozen sections of mouse kidney tissue were cut at 10-μm thickness from frozen blocks so as not to compromise the tdTomato signal. The sections were stained with LTA-Fluorescein, DAPI, and hematoxylin and eosin.

Imaging

All images were captured in tiff format and processed in Adobe Photoshop CS5.1. For immunofluorescence, Transwell-cultured MDCK cells were imaged on a Leica TCS SP5 confocal microscope with an HCX PL APO ×63/1.4–0.6 oil objective.

Nanoparticle tracking analysis

The nanoparticle tracking analysis was performed with the ZetaView Nanoparticle Tracking Analyzer, and the tracking parameters used were: camera sensitivity (85), shutter (250), frame rate (30f/s), minimum brightness(20), maximum size (1000), minimum size (8), and traces (12).

Electron microscopy (EM)

EM was used to observe EV morphology. The EV samples were prepared as described above. For EM, briefly, 4-μl drops of EVs in PBS were adsorbed on 300 mesh copper grids coated with formvar/carbon (catalog number FCF300-Cu, Electron Microscopy Sciences) for 1–5 min at room temperature, then the grid was rinsed gently with 5 drops of 5 mM Tris buffer, followed by 5 drops of distilled water. Samples were stained with 0.8% uranyl acetate (catalog number 22400, Electron Microscopy Sciences) for 30 s, followed by air drying for 30 min. EVs were examined at 80 kV with a Morgagni 268D transmission electron microscope (FEI, Brno, CZ) equipped with a MegaViewIII digital camera (Soft Imaging System).

Statistical analysis

Data were analyzed using Microsoft Excel for Mac (version 16.16.2), SAS software (version 9.4, SAS Institute, Cary, NC), and R software (version 3.6.0, R Core team, Vienna, Austria). Results were expressed as the mean ± S.D., unless otherwise specified. The Student's t test was applied to determine the significance of differences between treatment groups when observations were independent. Otherwise, linear mixed models were used to account for clustering within samples. All statistical tests were two-sided and unpaired. p values <0.05 were considered statistically significant.

For the MS data, the intensity values from the mass spectrometry analysis were converted to integers within Excel and read as raw (not normalized) values into the R package DESeq2 (64). DESeq2 is designed to account for biological dispersion among replicates in an experimental design and performs normalization of the data and computes a Benjamini-Hochberg False Discovery Rate correction on all p values for every protein in the analysis set (65). The Identity (Fig. 2*A*) and PCA (Fig. 2*B*) are standard plots from the DESeq2 package and offer a visual representation of the data groups. The Heatmap (Fig. 2*C*) was constructed with https://github.com/MUSC-CGM/sequencingHeatmap[3] using the unsupervised hierarchical clustering method of the gplots version 3.0.1 and default parameters. The protein expression data were clustered as shown by the y axis dendrograms whereas the x axis is ordered by experimental treatment.

Author contributions—X. Z., M. G. J., and Y. D. data curation; X. Z., S.-H. K., M. G. J., S. D. L., and J. H. L. formal analysis; X. Z. and Y. D. investigation; X. Z., S.-H. K., M. G. J., S. D. L., B. F., and N. P. writing-review and editing; J. H. L. conceptualization; J. H. L. supervision; J. H. L. funding acquisition; J. H. L. writing-original draft; J. H. L. project administration.

Acknowledgments—The UAB P30 Hepatorenal Fibrocystic Disease Core Center, supported by National Institutes of Health Grant P30DK074038, is acknowledged for generating the Exoc5fl/fl mouse line. Dr. Ben Humphreys is gratefully acknowledged for providing the SLC34A-CreERT2 mice. The Medical University of South Carolina Proteomics Center is acknowledged for performing MS. Dr. E. Starr Hazard is gratefully acknowledged for help with the proteomics data analysis.

References

1. The International Polycystic Kidney Disease Consortium (1995) Polycystic kidney disease: the complete structure of the PKD1 gene and its protein. *Cell* **81,** 289–298 CrossRef Medline
2. Hughes, J., Ward, C. J., Peral, B., Aspinwall, R., Clark, K., San Millán, J. L., Gamble, V., and Harris, P. C. (1995) The polycystic kidney disease 1 (PKD1) gene encodes a novel protein with multiple cell recognition domains. *Nat. Genet.* **10,** 151–160 CrossRef Medline
3. Yoder, B. K., Hou, X., and Guay-Woodford, L. M. (2002) The polycystic kidney disease proteins, polycystin-1, polycystin-2, polaris, and cystin, are co-localized in renal cilia. *J. Am. Soc. Nephrol.* **13,** 2508–2516 CrossRef Medline
4. Mochizuki, T., Wu, G., Hayashi, T., Xenophontos, S. L., Veldhuisen, B., Saris, J. J., Reynolds, D. M., Cai, Y., Gabow, P. A., Pierides, A., Kimberling, W. J., Breuning, M. H., Deltas, C. C., Peters, D. J., and Somlo, S. (1996) PKD2, a gene for polycystic kidney disease that encodes an integral membrane protein. *Science* **272,** 1339–1342 CrossRef Medline
5. Onuchic, L. F., Furu, L., Nagasawa, Y., Hou, X., Eggermann, T., Ren, Z., Bergmann, C., Senderek, J., Esquivel, E., Zeltner, R., Rudnik-Schöneborn, S., Mrug, M., Sweeney, W., Avner, E. D., Zerres, K., Guay-Woodford, L. M., Somlo, S., and Germino, G. G. (2002) PKHD1, the polycystic kidney and hepatic disease 1 gene, encodes a novel large protein containing multiple immunoglobulin-like plexin-transcription-factor domains and parallel beta-helix 1 repeats. *Am. J. Hum. Genet.* **70,** 1305–1317 CrossRef Medline
6. Ward, C. J., Hogan, M. C., Rossetti, S., Walker, D., Sneddon, T., Wang, X., Kubly, V., Cunningham, J. M., Bacallao, R., Ishibashi, M., Milliner, D. S., Torres, V. E., and Harris, P. C. (2002) The gene mutated in autosomal recessive polycystic kidney disease encodes a large, receptor-like protein. *Nat. Genet.* **30,** 259–269 CrossRef Medline
7. Ward, C. J., Yuan, D., Masyuk, T. V., Wang, X., Punyashthiti, R., Whelan, S., Bacallao, R., Torra, R., LaRusso, N. F., Torres, V. E., and Harris, P. C. (2003) Cellular and subcellular localization of the ARPKD protein: fibrocystin is expressed on primary cilia. *Hum. Mol. Genet.* **12,** 2703–2710 CrossRef Medline

[3] Please note that the JBC is not responsible for the long-term archiving and maintenance of this site or any other third party hosted site.

8. Hurd, T. W., and Hildebrandt, F. (2011) Mechanisms of nephronophthisis and related ciliopathies. *Nephron Exp. Nephrol.* **118,** e9–e14 CrossRef Medline
9. Grantham, J. J. (2001) Polycystic kidney disease: from the bedside to the gene and back. *Curr. Opin. Nephrol. Hypertens.* **10,** 533–542 CrossRef Medline
10. USRDS (2016) *Incidence, prevalence, patient characteristics, and treatment modalities*. Volume 2, Chapter 1, United States Renal Data System
11. Mathivanan, S., Ji, H., and Simpson, R. J. (2010) Exosomes: extracellular organelles important in intercellular communication. *J. Proteomics* **73,** 1907–1920 CrossRef Medline
12. Cocucci, E., Racchetti, G., and Meldolesi, J. (2009) Shedding microvesicles: artefacts no more. *Trends Cell Biol.* **19,** 43–51 CrossRef Medline
13. Mallegol, J., Van Niel, G., Lebreton, C., Lepelletier, Y., Candalh, C., Dugave, C., Heath, J. K., Raposo, G., Cerf-Bensussan, N., and Heyman, M. (2007) T84-intestinal epithelial exosomes bear MHC class II/peptide complexes potentiating antigen presentation by dendritic cells. *Gastroenterology* **132,** 1866–1876 CrossRef Medline
14. Al-Nedawi, K., Meehan, B., Micallef, J., Lhotak, V., May, L., Guha, A., and Rak, J. (2008) Intercellular transfer of the oncogenic receptor EGFRvIII by microvesicles derived from tumour cells. *Nat. Cell Biol.* **10,** 619–624 CrossRef Medline
15. Camici, M. (2008) Urinary biomarkers of podocyte injury. *Biomark Med.* **2,** 613–616 CrossRef Medline
16. Cheruvanky, A., Zhou, H., Pisitkun, T., Kopp, J. B., Knepper, M. A., Yuen, P. S., and Star, R. A. (2007) Rapid isolation of urinary exosomal biomarkers using a nanomembrane ultrafiltration concentrator. *Am. J. Physiol. Renal Physiol.* **292,** F1657–F1661 CrossRef Medline
17. D'Souza-Schorey, C., and Clancy, J. W. (2012) Tumor-derived microvesicles: shedding light on novel microenvironment modulators and prospective cancer biomarkers. *Genes Dev.* **26,** 1287–1299 CrossRef Medline
18. Pisitkun, T., Johnstone, R., and Knepper, M. A. (2006) Discovery of urinary biomarkers. *Mol. Cell. Proteomics* **5,** 1760–1771 CrossRef Medline
19. Wood, C. R., Huang, K., Diener, D. R., and Rosenbaum, J. L. (2013) The cilium secretes bioactive ectosomes. *Curr. Biol.* **23,** 906–911 CrossRef Medline
20. Barr, M. M., and Sternberg, P. W. (1999) A polycystic kidney-disease gene homologue required for male mating behaviour in *C. elegans*. *Nature* **401,** 386–389 CrossRef Medline
21. Wang, J., Silva, M., Haas, L. A., Morsci, N. S., Nguyen, K. C., Hall, D. H., and Barr, M. M. (2014) *C. elegans* ciliated sensory neurons release extracellular vesicles that function in animal communication. *Curr. Biol.* **24,** 519–525 CrossRef Medline
22. Nager, A. R., Goldstein, J. S., Herranz-Pérez, V., Portran, D., Ye, F., Garcia-Verdugo, J. M., and Nachury, M. V. (2017) An actin network dispatches ciliary GPCRs into extracellular vesicles to modulate signaling. *Cell* **168,** 252–263.e214 CrossRef Medline
23. Hsu, S. C., Ting, A. E., Hazuka, C. D., Davanger, S., Kenny, J. W., Kee, Y., and Scheller, R. H. (1996) The mammalian brain rsec6/8 complex. *Neuron* **17,** 1209–1219 CrossRef Medline
24. Novick, P., Field, C., and Schekman, R. (1980) Identification of 23 complementation groups required for post-translational events in the yeast secretory pathway. *Cell* **21,** 205–215 CrossRef Medline
25. Lipschutz, J. H., and Mostov, K. E. (2002) Exocytosis: the many masters of the exocyst. *Curr. Biol.* **12,** R212–R214 CrossRef Medline
26. Rogers, K. K., Wilson, P. D., Snyder, R. W., Zhang, X., Guo, W., Burrow, C. R., and Lipschutz, J. H. (2004) The exocyst localizes to the primary cilium in MDCK cells. *Biochem. Biophys. Res. Commun.* **319,** 138–143 CrossRef Medline
27. Zuo, X., Guo, W., and Lipschutz, J. H. (2009) The exocyst protein Sec10 is necessary for primary ciliogenesis and cystogenesis *in vitro*. *Mol. Biol. Cell* **20,** 2522–2529 CrossRef Medline
28. Choi, S. Y., Chacon-Heszele, M. F., Huang, L., McKenna, S., Wilson, F. P., Zuo, X., and Lipschutz, J. H. (2013) Cdc42 deficiency causes ciliary abnormalities and cystic kidneys. *J. Am. Soc. Nephrol.* **24,** 1435–1450 CrossRef Medline
29. Fogelgren, B., Lin, S. Y., Zuo, X., Jaffe, K. M., Park, K. M., Reichert, R. J., Bell, P. D., Burdine, R. D., and Lipschutz, J. H. (2011) The exocyst protein Sec10 interacts with polycystin-2 and knockdown causes PKD-phenotypes. *PLoS Genet.* **7,** e1001361 CrossRef Medline
30. Fogelgren, B., Polgar, N., Lui, V. H., Lee, A. J., Tamashiro, K. K., Napoli, J. A., Walton, C. B., Zuo, X., and Lipschutz, J. H. (2015) Urothelial defects from targeted inactivation of exocyst Sec10 in mice cause ureteropelvic junction obstructions. *PLoS ONE* **10,** e0129346 CrossRef Medline
31. Polgar, N., Lee, A. J., Lui, V. H., Napoli, J. A., and Fogelgren, B. (2015) The exocyst gene Sec10 regulates renal epithelial monolayer homeostasis and apoptotic sensitivity. *Am. J. Physiol. Cell Physiol.* **309,** C190–C201 CrossRef Medline
32. Fogelgren, B., Zuo, X., Buonato, J. M., Vasilyev, A., Baek, J. I., Choi, S. Y., Chacon-Heszele, M. F., Palmyre, A., Polgar, N., Drummond, I., Park, K. M., Lazzara, M. J., and Lipschutz, J. H. (2014) Exocyst Sec10 protects renal tubule cells from injury by EGFR/MAPK activation and effects on endocytosis. *Am. J. Physiol. Renal Physiol.* **307,** F1334–F1341 CrossRef Medline
33. Ren, J., and Guo, W. (2012) ERK1/2 regulate exocytosis through direct phosphorylation of the exocyst component Exo70. *Dev. Cell* **22,** 967–978 CrossRef Medline
34. Zuo, X., Lobo, G., Fulmer, D., Guo, L., Dang, Y., Su, Y., Ilatovskaya, D. V., Nihalani, D., Rohrer, B., Body, S. C., Norris, R. A., and Lipschutz, J. H. (2019) The exocyst acting through the primary cilium is necessary for renal ciliogenesis, cystogenesis, and tubulogenesis. *J. Biol. Chem.* **294,** 6710–6718 CrossRef Medline
35. Dixon-Salazar, T. J., Silhavy, J. L., Udpa, N., Schroth, J., Bielas, S., Schaffer, A. E., Olvera, J., Bafna, V., Zaki, M. S., Abdel-Salam, G. H., Mansour, L. A., Selim, L., Abdel-Hadi, S., Marzouki, N., Ben-Omran, T., *et al.* (2012) Exome sequencing can improve diagnosis and alter patient management. *Sci. Transl. Med.* **4,** 138ra178 Medline
36. Chacon-Heszele, M. F., Choi, S. Y., Zuo, X., Baek, J. I., Ward, C., and Lipschutz, J. H. (2014) The exocyst and regulatory GTPases in urinary exosomes. *Physiol. Rep.* **2,** e12116 CrossRef Medline
37. Prigent, M., Dubois, T., Raposo, G., Derrien, V., Tenza, D., Rossé, C., Camonis, J., and Chavrier, P. (2003) ARF6 controls post-endocytic recycling through its downstream exocyst complex effector. *J. Cell Biol.* **163,** 1111–1121 CrossRef Medline
38. Hogan, M. C., Manganelli, L., Woollard, J. R., Masyuk, A. I., Masyuk, T. V., Tammachote, R., Huang, B. Q., Leontovich, A. A., Beito, T. G., Madden, B. J., Charlesworth, M. C., Torres, V. E., LaRusso, N. F., Harris, P. C., and Ward, C. J. (2009) Characterization of PKD protein-positive exosome-like vesicles. *J. Am. Soc. Nephrol* **20,** 278–288 CrossRef Medline
39. Liu, Q., Tan, G., Levenkova, N., Li, T., Pugh, E. N., Jr., Rux, J. J., Speicher, D. W., and Pierce, E. A. (2007) The proteome of the mouse photoreceptor sensory cilium complex. *Mol. Cell. Proteomics* **6,** 1299–1317 CrossRef Medline
40. Grindstaff, K. K., Yeaman, C., Anandasabapathy, N., Hsu, S. C., Rodriguez-Boulan, E., Scheller, R. H., and Nelson, W. J. (1998) Sec6/8 complex is recruited to cell-cell contacts and specifies transport vesicle delivery to the basal-lateral membrane in epithelial cells. *Cell* **93,** 731–740 CrossRef Medline
41. Lipschutz, J. H., Guo, W., O'Brien, L. E., Nguyen, Y. H., Novick, P., and Mostov, K. E. (2000) Exocyst is involved in cystogenesis and tubulogenesis and acts by modulating synthesis and delivery of basolateral plasma membrane and secretory proteins. *Mol. Biol. Cell* **11,** 4259–4275 CrossRef Medline
42. Lipschutz, J. H., Lingappa, V. R., and Mostov, K. E. (2003) The exocyst affects protein synthesis by acting on the translocation machinery of the endoplasmic reticulum. *J. Biol. Chem.* **278,** 20954–20960 CrossRef Medline
43. Toikkanen, J. H., Miller, K. J., Söderlund, H., Jäntti, J., and Keränen, S. (2003) The β subunit of the Sec61p ER translocon interacts with the exocyst complex in saccharomyces cerevisiae. *J. Biol. Chem.* **278,** 20946–20953 CrossRef Medline
44. Yoder, B. K., Tousson, A., Millican, L., Wu, J. H., Bugg, C. E., Jr., Schafer, J. A., and Balkovetz, D. F. (2002) Polaris, a protein disrupted in orpk mu-

tant mice, is required for assembly of renal cilium. *Am. J. Physiol. Renal Physiol.* **282,** F541–F552 CrossRef Medline
45. Kusaba, T., Lalli, M., Kramann, R., Kobayashi, A., and Humphreys, B. D. (2014) Differentiated kidney epithelial cells repair injured proximal tubule. *Proc. Natl. Acad. Sci. U.S.A.* **111,** 1527–1532 CrossRef Medline
46. Lobo, G. P., Fulmer, D., Guo, L., Zuo, X., Dang, Y., Kim, S. H., Su, Y., George, K., Obert, E., Fogelgren, B., Nihalani, D., Norris, R. A., Rohrer, B., and Lipschutz, J. H. (2017) The exocyst is required for photoreceptor ciliogenesis and retinal development. *J. Biol. Chem.* **292,** 14814–14826 CrossRef Medline
47. Delling, M., DeCaen, P. G., Doerner, J. F., Febvay, S., and Clapham, D. E. (2013) Primary cilia are specialized calcium signalling organelles. *Nature* **504,** 311–314 CrossRef Medline
48. Guo, W., Roth, D., Walch-Solimena, C., and Novick, P. (1999) The exocyst is an effector for Sec4p, targeting secretory vesicles to sites of exocytosis. *EMBO J.* **18,** 1071–1080 CrossRef Medline
49. Seixas, C., Choi, S. Y., Polgar, N., Umberger, N. L., East, M. P., Zuo, X., Moreiras, H., Ghossoub, R., Benmerah, A., Kahn, R. A., Fogelgren, B., Caspary, T., Lipschutz, J. H., and Barral, D. C. (2016) Arl13b and the exocyst interact synergistically in ciliogenesis. *Mol. Biol. Cell* **27,** 308–320 CrossRef Medline
50. Choi, S. Y., Baek, J. I., Zuo, X., Kim, S. H., Dunaief, J. L., and Lipschutz, J. H. (2015) Cdc42 and sec10 are required for normal retinal development in zebrafish. *Invest. Ophthalmol. Vis. Sci.* **56,** 3361–3370 CrossRef Medline
51. Zhang, X., Bi, E., Novick, P., Du, L., Kozminski, K. G., Lipschutz, J. H., and Guo, W. (2001) Cdc42 interacts with the exocyst and regulates polarized secretion. *J. Biol. Chem.* **276,** 46745–46750 CrossRef Medline
52. Brymora, A., Valova, V. A., Larsen, M. R., Roufogalis, B. D., and Robinson, P. J. (2001) The brain exocyst complex interacts with RalA in a GTP-dependent manner: identification of a novel mammalian Sec3 gene and a second Sec15 gene. *J. Biol. Chem.* **276,** 29792–29797 CrossRef Medline
53. Moskalenko, S., Henry, D. O., Rosse, C., Mirey, G., Camonis, J. H., and White, M. A. (2002) The exocyst is a Ral effector complex. *Nat. Cell Biol.* **4,** 66–72 CrossRef Medline
54. Polzin, A., Shipitsin, M., Goi, T., Feig, L. A., and Turner, T. J. (2002) Ral-GTPase influences the regulation of the readily releasable pool of synaptic vesicles. *Mol. Cell. Biol.* **22,** 1714–1722 CrossRef Medline
55. Sugihara, K., Asano, S., Tanaka, K., Iwamatsu, A., Okawa, K., and Ohta, Y. (2002) The exocyst complex binds the small GTPase RalA to mediate filopodia formation. *Nat. Cell Biol.* **4,** 73–78 CrossRef Medline
56. Baek, J. I., Kwon, S. H., Zuo, X., Choi, S. Y., Kim, S. H., and Lipschutz, J. H. (2016) Dynamin binding protein (Tuba) deficiency inhibits ciliogenesis and nephrogenesis *in vitro* and *in vivo*. *J. Biol. Chem.* **291,** 8632–8643 CrossRef Medline
57. DeLay, B. D., Baldwin, T. A., and Miller, R. K. (2019) Dynamin binding protein is required for *Xenopus laevis* kidney development. *Front. Physiol.* **10,** 143 CrossRef Medline
58. Zuo, X., Fogelgren, B., and Lipschutz, J. H. (2011) The small GTPase Cdc42 is necessary for primary ciliogenesis in renal tubular epithelial cells. *J. Biol. Chem.* **286,** 22469–22477 CrossRef Medline
59. Hogan, M. C., Johnson, K. L., Zenka, R. M., Charlesworth, M. C., Madden, B. J., Mahoney, D. W., Oberg, A. L., Huang, B. Q., Leontovich, A. A., Nesbitt, L. L., Bakeberg, J. L., McCormick, D. J., Bergen, H. R., and Ward, C. J. (2014) Subfractionation, characterization, and in-depth proteomic analysis of glomerular membrane vesicles in human urine. *Kidney Int.* **85,** 1225–1237 CrossRef Medline
60. León, I. R., Schwämmle, V., Jensen, O. N., and Sprenger, R. R. (2013) Quantitative assessment of in-solution digestion efficiency identifies optimal protocols for unbiased protein analysis. *Mol. Cell. Proteomics* **12,** 2992–3005 CrossRef Medline
61. Benjamini, Y., and Hochberg, Y. (1995) Controlling the false discovery rate: a practical and powerful approach to multiple testing. *J. R. Statist. Soc. B* **57,** 289–300
62. Anders, S., and Huber, W. (2010) Differential expression analysis for sequence count data. *Genome Biol.* **11,** R106 CrossRef Medline
63. Anders, S., McCarthy, D. J., Chen, Y., Okoniewski, M., Smyth, G. K., Huber, W., and Robinson, M. D. (2013) Count-based differential expression analysis of RNA sequencing data using R and Bioconductor. *Nat. Protoc.* **8,** 1765–1786 CrossRef Medline
64. Love, M. I., Huber, W., and Anders, S. (2014) Moderated estimation of fold change and dispersion for RNA-seq data with DESeq2. *Genome Biol.* **15,** 550 CrossRef Medline
65. Hochberg, Y., and Benjamini, Y. (1990) More powerful procedures for multiple significance testing. *Stat. Med.* **9,** 811–818 CrossRef Medline